

Brugada syndrome trafficking-defective Nav1.5 channels can trap cardiac Kir2.1/2.2 channels

Marta Pérez-Hernández,^{#1} Marcos Matamoros,^{#1} Silvia Alfayate,¹ Paloma Nieto-Marín,¹ Raquel G. Utrilla,¹ David Tinaquero,¹ Raquel de Andrés,² Teresa Crespo,¹ Daniela Ponce-Balbuena,³ B. Cicero Willis,³ Eric N. Jiménez-Vázquez,³ Guadalupe Guerrero-Serna,³ Andre M. da Rocha,³ Katherine Campbell,³ Todd J. Herron,³ F. Javier Díez-Guerra,² Juan Tamargo,¹ José Jalife,^{3,4} Ricardo Caballero,^{1†*} Eva Delpón^{1†}

SUPPLEMENTAL MATERIAL

Supplemental Methods

Kir2.x and Nav1.5 constructs and Chinese hamster ovary (CHO) cell transfection.

Human Kir2.1 (NM_000891.2), Kir2.2 (NM_021012.4) (Origene, USA) and Kir2.3 (NM_004981.1) (kindly provided by Dr. José Antonio Sánchez Chapula; Colima University, Mexico) were subcloned into pcDNA3.1 plasmid (Invitrogen). Human cardiac Nav1.5 (hH1; NM_198056.2) and Navβ1 (NM_001037.4) cDNA subcloned in pCGI vector (which includes GFP) were kindly gifted by Dr. Connie R. Bezzina (University of Amsterdam, The Netherlands). Nav1.5 mutants were made by using the QuikChange Site-Directed Mutagenesis kit (Stratagene, USA) (1-4). All mutations were confirmed by direct DNA sequencing. CHO cell were purchased from ATCC and mycoplasma contamination was discarded by specific testing. CHO cells were cultured

as previously described (1-8) and transiently transfected with the cDNA encoding WT or mutated Nav1.5 channels (1.6 µg) and hNavβ1 (1.6 µg) (Nav1.5-β) alone or together with WT Kir2.x (1.6 µg) plus the cDNA encoding the CD8 antigen (0.5 µg) by using FUGENE XtremeGENE (Roche Diagnostics, Switzerland) following manufacturer instructions. 48 h after transfection, cells were incubated with polystyrene microbeads precoated with anti-CD8 antibody (Dynabeads M450; Life Technologies). Most of the cells that were beaded also had channel expression. Coexpression of Nav1.5 and Kir2.x channels was always tested electrophysiologically and by fluorescence detection, and only cells coexpressing both channels were patched. In some experiments, CHO transfected cells were incubated for 24 h at room temperature (2,3) or in the presence of 4-phenylbutyrate (5 mM) (2,3) or brefeldin-A (BFA, 50 ng/mL). In other groups of experiments, WT and mutant Nav1.5 channels were cotransfected with MOG1 (1.6 µg) or GRASP55 (1.6 µg).

Rat ventricular myocyte isolation.

Single ventricular myocytes were isolated from hearts of male Sprague–Dawley rats (225 to 250 g) by enzymatic dissociation with collagenase type II (Worthington) following previously described methods (1,4). Rats were heparinized (1.000 U/kg i.p.) and anesthetized with sodium pentobarbital (50 mg/kg i.p.). After myocyte isolation, cell pellet was resuspended in Medium 199 (M199; Sigma) supplemented with 5% fetal bovine serum (Invitrogen, USA), 0.68 mM L-glutamine (Invitrogen, USA), 10 mM reduced L-glutathione (Sigma), 3 mM bovine serum albumin (BSA; Sigma), 680 µM L-glutamine, and 100 U/mL penicillin and 100 µg/mL streptomycin. Thereafter, myocytes were seeded on laminin-coated glass coverslips and infected with adenoviral constructs encoding for human Nav1.5 either WT or mutated two hours after plating (1,4).

Multiplicity of infection (MOI) of 75, 200, 150, 120, and 350 were used for GFP, Nav1.5 WT, p.D1690N, p.G1748D, and p.D1816VfsX7, respectively. The same stock of adenovirus was used for all of the experiments. Currents were recorded 48 h after the infection.

Mouse ventricular myocyte isolation.

Single ventricular myocytes were isolated from 3-4 month old male heterozygous *KCNJ2*-overexpressing (*Kcnj2OE*^{+/-}) mice (9), heterozygous knockout *SCN5A* (*Scn5a*^{+/-}) mice, or a double mutant resulting from the cross-bred of both mice (*Kcnj2OE*^{+/-}-*Scn5a*^{+/-}). *Scn5a*^{+/-} mice, constructed by using Cre-recombinase mediated cassette exchange with GFP in the targeted locus (10), were kindly provided by Prof. Dan Roden (Vanderbilt University, Nashville, TN, USA) and recapitulate most of the features of the Brugada syndrome (11). Supplemental Figure 1A shows an end-point PCR agarose gel of WT and *Kcnj2OE*^{+/-}-*Scn5a*^{+/-} mouse profiles obtained when successfully cross-breeding *Scn5a*^{+/-} and *Kcnj2OE*^{+/-} mice. The genetic distribution was that of Mendelian inheritance with a 25% probability of obtaining each of the four groups with no evidence of embryonic death (Supplemental Figure 1B). Control experiments were conducted in myocytes isolated from the corresponding WT littermates. Myocytes were isolated following previously described methods (12). Briefly, mice were heparinized (1,000 IU/mL i.p.) and then anesthetized with Ketamine and Xylazin or euthanized by a CO₂ overdose. Cells were used for electrophysiological recording within 8 h of isolation. Detection of Nav1.5 and Kir2.1 proteins was carried out in ventricular samples from WT, *Kcnj2OE*^{+/-}, *Scn5a*^{+/-}, and *Kcnj2OE*^{+/-}-*Scn5a*^{+/-} mice by Western-blot following previously described procedures (12). Mouse ventricle tissue samples were washed with PBS containing protease inhibitors (Roche) and flash

frozen in liquid nitrogen. Frozen tissues were homogenized in lysis buffer (mM): Tris.HCl 25, NaCl 150, EDTA 1, NaF 2, Na ortho-vanadate 2, Triton X-100 1% and protease inhibitors (Roche). The homogenates were centrifuged at 10,000 rpm for 10 minutes; the supernatants were used for western blotting. Protein concentrations were determined using a Bradford protein concentration assay (Bio-Rad). Tissue lysates (50 µg) were then subjected to one-dimensional sodium dodecyl sulfate polyacrylamide gel electrophoresis, using 4-20% Tris-Glycine Novex gels (Thermo-Fisher Scientific) and transferred to nitrocellulose membranes (Bio-Rad) using a Hoefer transfer apparatus (Holliston, MA, USA). Nonspecific binding sites were blocked with 5% nonfat dry milk in PBS with Tween-20 (0.05%). Membranes were then incubated with specific primary antibodies diluted in 5% nonfat dry milk overnight at 4 °C. After washing, membranes were incubated with peroxidase-conjugated secondary antibodies (Jackson Immunoresearch, West Grove, PA, USA). Primary antibodies used: rabbit GAPDH (G9545; 1:5000, Sigma-Aldrich, St. Louis, MO), rabbit Nav1.5 (ASC-005) and Kir2.1 (APC-026) (both at 1:500, Alomone Labs, Jerusalem, Israel). The protein bands were visualized using Supersignal chemiluminescence (Pierce Biotechnology Inc, Rockford, IL) and imaged using Image Lab software 5 (Bio-Rad). Densities of protein bands were measured using Image Lab software 5.

Patch-clamping (1-8,12).

Currents were recorded at room temperature (21-23°C) using the whole-cell patch-clamp technique using an Axopatch-200B patch clamp amplifier (Molecular Devices, USA). Recording pipettes were pulled from 1.0 mm o.d. borosilicate capillary tubes (GD1, Narishige Co., Ltd, Japan) using a programmable patch micropipette puller (Model P-2000 Brown-Flaming, Sutter Instruments Co., USA) and were heat-polished

with a microforge (Model MF-83, Narishige). Micropipette resistance was kept below 3.5 MΩ when filled with the internal solution and immersed in the external solution. In all experiments, series resistance was compensated manually by using the series resistance compensation unit of the Axopatch amplifier, and ≥80% compensation was achieved. Uncompensated access resistance and cell capacitance were 1.87±0.9 MΩ and 9.76±0.3 pF (n=168178), 3.12±1.4 MΩ and 120118.19±2.6 pF (n=252324), and 2.0±0.3 MΩ and 155.4±8.5 pF (n=65) in CHO, rat and mouse ventricular myocardial cells, respectively. Under our experimental conditions no significant voltage errors (<5 mV) due to series resistance were expected with the micropipettes used.

To record I_{K1} in cultured rat ventricular myocytes, the external solution contained (mM): NaCl 120, KCl 20, CaCl₂ 1, MgCl₂ 1, HEPES 10, 4-aminopyridine 2, glucose 10, nifedipine (1 μM), atropine (1 μM), and glibenclamide (10 μM) (pH 7.4 with NaOH). Recording pipettes were filled with an internal solution containing (mM): K-aspartate 80, KCl 42, KH₂PO₄ 10, MgATP 5, phosphocreatine 3, HEPES 5, and EGTA 5 (pH 7.2 with KOH). The liquid junction potential (LJP) between the pipette and external solution was -12 mV. To record I_{K1} in mouse ventricular myocytes, the external solution contained (mM): NaCl 143.4, NaH₂PO₄ 0.4, MgCl₂ 1, KCl 10, CaCl₂ 1, HEPES 15, glucose 10, and nifedipine (1 μM) (pH=7.4 with NaOH). BaCl₂ (1 mM) was used to isolate I_{K1} from other background currents. Recording pipettes were filled with an internal solution containing (mM): KCl 148, MgCl₂ 1, EGTA 5, HEPES 5, creatine 2, ATP 5, phosphocreatine 5 (pH 7.2 with KOH) (LJP=-4.1 mV). To record I_{Na} in cultured rat ventricular myocytes the external solution contained (mM): NaCl 4, CsCl 133.5, CaCl₂ 1, MgCl₂ 1, CdCl₂ 0.1, HEPES 20, and glucose 10 (pH 7.4 with CsOH). Recording pipettes were filled with an internal solution containing (mM): NaF 10, CsF 110, CsCl 20, HEPES 10, and EGTA 10 (pH 7.35 with CsOH). To record I_{Na} in mouse

ventricular myocytes, the external solution contained (mM): NaCl 5, $MgCl_2$ 1, $CaCl_2$ 1, $CdCl_2$ 0.1, CsCl 132.5, HEPES 20, and glucose 11 (pH 7.35 with CsOH), whereas internal solution contained (mM): NaCl 5, CsF 135, EGTA 10, MgATP 5, and HEPES 5 (pH 7.2 with CsOH). To record action potentials in cultured rat ventricular myocytes the external solution contained (mM): NaCl 136, KCl 4, $CaCl_2$ 1.8, $MgCl_2$ 1, HEPES 10, and glucose 10 (pH 7.4 with NaOH). The internal solution contained (mM): K-aspartate 80, KCl 42, KH_2PO_4 10, MgATP 5, phosphocreatine 3, HEPES 5, and EGTA 5 (pH=7.2 with KOH).

To record $I_{Kir2.x}$ and $I_{Nav1.5}$, CHO cells were perfused with an external solution containing (mM): NaCl 136, KCl 4, $CaCl_2$ 1.8, $MgCl_2$ 1, HEPES 10, and glucose 10 (pH 7.4 with NaOH). Recording pipettes were filled with an internal solution containing (mM): K-aspartate 80, KCl 42, KH_2PO_4 10, MgATP 5, phosphocreatine 3, HEPES 5, and EGTA 5 (pH 7.2 with KOH) to record $I_{Kir2.x}$ (LJP=-13.2 mV) or NaF 10, CsF 110, CsCl 20, HEPES 10, and EGTA 10 (pH 7.35 with CsOH) to record $I_{Nav1.5}$. I_{K1} and $I_{Kir2.x}$ current-voltage (I-V) curves were corrected according to the calculated LJP between the pipette and external solution (1,4-8). To minimize the contribution of time-dependent shifts of channel availability during sodium current recordings, all data were collected 20 min after establishing the whole-cell configuration. Under these conditions current amplitudes and voltage dependence of activation and inactivation were stable during the time of recordings (1-3).

Pulse protocols and analysis (1-8,12).

I_{Na} in rat ventricular myocytes was recorded by applying 20-ms pulses in 5 mV increments from a holding potential of -120 mV to potentials ranging -90 and +30 mV.

Conductance-voltage curves for I_{Na} were constructed by plotting the normalized

conductance as a function of the membrane potential. The conductance was estimated for each experiment by the equation:

$$G=I/(V_m-E_{rev})$$

where G is the conductance at the test potential V_m , I represents the peak maximum current at V_m , and E_{rev} is the reversal potential. To determine the E_{rev} ,

I_{Na} density-voltage relationships obtained in each experiment were fitted to a function

of the form:

$$I=(V_m-E_{rev})*G_{max}*(1+\exp[V_m-V_h]/k)^{-1}$$

where I is the peak current elicited at the test potential V_m , G_{max} is the maximum conductance, and k is the slope factor.

To construct the inactivation curves, currents were recorded by applying 500-ms pulses from -120 mV to potentials between -140 and -20 mV in 10 mV increments followed by a test pulse to -20 mV. Availability curves were constructed by plotting the current amplitude recorded with the test pulse at -20 mV as a function of the membrane potential of the preceding pulse. A Boltzmann function was fitted to activation/conductance-voltage and inactivation curves to obtain the midpoint (V_h) and the slope (k) values of the curves. In mouse ventricular myocytes, I_{Na} was recorded by applying 200-ms pulses from -120 mV to potentials ranging -100 and $+30$ mV in 5 mV steps.

The protocol to record $I_{Nav1.5}$ consisted of 50-ms pulses in 5 mV increments from -120 mV to potentials between -80 and $+50$ mV.

The protocol to record rat ventricular I_{K1} consisted of 250-ms steps that were imposed in 10 mV increments from -40 mV to potentials ranging -100 and $+30$ mV. In mouse ventricular myocytes, I_{K1} was recorded by applying 400-ms pulses from a holding potential of -50 mV to potentials between -120 and $+30$ mV in 10 mV steps. For $I_{Kir2.x}$, the protocol to obtain I-V curves consisted of 250-ms pulses in 10 mV increments from

–60 mV to potentials between –120 and +20 mV. Current amplitude was measured at the end of the pulse.

$I_{Kir2.x}/I_{K1}$ and $I_{Nav1.5}/I_{Na}$ recordings were sampled at 4 and 50 kHz, respectively, filtered at half the sampling frequency, and stored on the hard disk of a computer for subsequent analysis. Data were analyzed using pCLAMP software (Molecular Devices).

In each experiment, current amplitudes were normalized to membrane capacitance to obtain current densities.

Action potentials were recorded in cultured rat ventricular myocytes using the current clamp configuration and elicited by depolarizing-current pulses of 2 ms in duration at 1.5 times the current threshold at a frequency of 1 Hz.

I_{Na} , I_{K1} , and action potentials recordings in human induced pluripotent stem cell-derived cardiomyocytes (hiPSC-CMs).

DF19-9-11T hiPSC-CMs line was derived from foreskin fibroblasts without integration of vector and transgene sequences (4,13). DF19-9-11T hiPSC-CMs were plated on Matrigel-coated (500 μ g/mL; BD Biosciences, San Jose, CA) transparent polydimethylsiloxane (PDMS) membranes for cardiac directed differentiation as previously described (4,13). Differentiation medium (EB-20) consisted of 80% DMEM/F12, 0.1 mM β -mercaptoethanol, 20% FBS, and 10 μ M blebbistatin. Thirty days after differentiation, cells were purified using a Mitenyi Biotec kit (PSC-Derived Cardiomyocyte Isolation Kit, human) and seeded again on PDMS-matrigel coverslips (4,13). One week later, cells were infected with the adenoviral constructs encoding Nav1.5 WT (Ad-Nav1.5) or p.G1748D (Ad-p.G1748D) (MOI=10 each). In each case, the same stock of adenovirus was used for all of the experiments. Infection with Ad-Nav1.5 (64.5 \pm 7.9 pF) and Ad-p.G1748D (66.5 \pm 10.3 pF) did not modify hiPSC-CM

capacitance (67.6 ± 13.4 pF) ($n=52$, $P > 0.05$). Currents and action potentials were recorded 72 h after the infection at room temperature (21-23°C) and at 35°C, respectively, using the whole-cell patch-clamp technique and a MultiClamp 700B amplifier (Molecular Devices, USA). Recording pipettes were pulled using a programmable patch micropipette puller (Model P-97 Brown-Flaming, Sutter Instruments Co.) and were heat-polished with a microforge (Model MF-83, Narishige). Micropipette resistance was kept below 3.5 M Ω for current recordings or between 4 and 6 M Ω for action potential recordings. In all experiments, series resistance and cell capacitance were compensated automatically. The external solution for I_{Na} recordings contained (mM): NaCl 50, MgCl₂ 1, CaCl₂ 1.8, CdCl₂ 0.1, CsCl 102.5, HEPES 20, and glucose 11 (pH= 7.35 with CsOH). Recording pipettes were filled with an internal solution containing (mM): NaCl 5, CsF 135, EGTA 10, Mg-ATP 5, and HEPES 5 (pH=7.2 with CsOH). The protocol to record I_{Na} consisted of 100-ms pulses from -160 mV to potentials ranging -80 and +45 mV in 5 mV steps.

The external solution for I_{K1} recordings contained (mM): NaCl 148, MgCl₂ 1, CaCl₂ 1.8, KCl 5.4, NaH₂PO₄ 0.4, HEPES 15, glucose 11 and nifedipine (5 μ M) (pH= 7.35 with NaOH). Recording pipettes were filled with an internal solution containing (mM): KCl 148, MgCl₂ 1, EGTA 5, Creatine 2, Mg-ATP 5, Phosphocreatine 5, HEPES 5 (pH=7.2 with KOH) (LJP=-4.3 mV). The protocol to record I_{K1} consisted of 400-ms pulses from -50 to potentials ranging -120 and +40 mV in 10 mV steps. These experiments were conducted in hiPSC-CMs seeded in coverslips. Since the effects of BaCl₂ are not fully reversible and the number of infected dishes limited, we decided not to use this compound to isolate I_{K1} and, thus, the total K⁺ current was recorded.

To record action potentials the external solution contained (mM) (4,7,13): NaCl 148, NaH₂PO₄ 0.4, MgCl₂ 1, glucose 5.5, KCl 5.4, HEPES 15, and CaCl₂ 1.8 (pH 7.4 with

NaOH), whereas the internal solution contained (mM): KCl 150, K_2ATP 4.46, phosphocreatine 5, HEPES 5, EGTA 1, $MgCl_2$ 1, and β -hydroxybutyric acid 2 (pH 7.2 with KOH). Cells were stimulated at 1 Hz in current-clamp configuration, using square wave pulses (amplitude 30-50 pA; duration 4 ms) generated by a DS8000 digital stimulator (World Precision Instruments, USA).

In different groups of experiments, currents and action potentials were recorded in iCell Cardiomyocytes2® (iCell²®) (Cellular Dynamics, USA) hiPSC-CM that were thawed and cultured in glass coverslips coated with 0.1% gelatin following the manufacturer's instructions. One week after thawing, cells were infected with the adenoviral constructs encoding Nav1.5 WT or p.D1690N (MOI=10 each). Another batch of iCell²® was transfected or not with the cDNA encoding p.R878C Nav1.5 (1 μ g) by using Viafect transfection reagent (Promega, USA). Adenoviral infection (45.3 ± 3.5 pF) or cDNA transfection (41.2 ± 2.8 pF) did not modify hiPSC-CM capacitance (39.4 ± 2.7 pF) ($n=289$, $P>0.05$). Currents and action potentials were recorded 48 h after the infection at room temperature (21-23°C) using the whole-cell patch-clamp technique and Axopatch 200B amplifiers. Micropipette resistance was kept below 3.5 M Ω for current recordings or between 4 and 6 M Ω for action potential recordings. In all experiments, series resistance and cell capacitance were compensated manually as mentioned above. The external solution for I_{Na} recordings contained (mM): NaCl 20, $MgCl_2$ 1.5, $CaCl_2$ 1, CsCl 115, HEPES 5, glucose 10 and nifedipine (1 μ M) (pH= 7.35 with CsOH). Recording pipettes were filled with an internal solution containing (mM): NaF 10, CsF 110, EGTA 10, CsCl 20, and HEPES 10 (pH=7.35 with CsOH). The protocol to record I_{Na} consisted of 50-ms pulses from -120 mV to potentials ranging -90 and +40 mV in 5 mV steps. The external solution for I_{K1} recordings contained (mM): NaCl 148, $MgCl_2$ 1, $CaCl_2$ 1.8, KCl 5.4, NaH_2PO_4 0.4, HEPES 15, glucose 11 and nifedipine (1 μ M) (pH= 7.35

with NaOH). Recording pipettes were filled with an internal solution containing (mM): KCl 148, MgCl₂ 1, EGTA 5, Creatine 2, Mg-ATP 5, Phosphocreatine 5, HEPES 5 (pH=7.2 with KOH). The protocol to record I_{K1} consisted of 250-ms pulses from -40 to potentials ranging -120 and +40 mV in 10 mV steps.

To record action potentials the external solution contained (mM): NaCl 148, NaH₂PO₄ 0.4, MgCl₂ 1, glucose 5.5, KCl 4.5, HEPES 15, and CaCl₂ 1.8 (pH 7.4 with NaOH), whereas the internal solution contained (mM): K-aspartate 80, KCl 42, KH₂PO₄ 10, MgATP 5, phosphocreatine 3, HEPES 5, and EGTA 5 (pH 7.2 with KOH). Spontaneous action potentials and action potentials elicited by depolarizing-current pulses of 2 ms in duration at 1.5-2 times the current threshold at a frequency of 1 Hz were recorded in the current-clamp configuration.

GRASP55/65 silencing in CHO cells, rat ventricular and hiPSC-derived cardiomyocytes (1).

For GRASP55 (Acc. No. XM_007611693.2) silencing, CHO cells were transfected with two different siRNA duplexes (siRNA1 and siRNA2 at 100 nM) or with siRNA Universal Negative Control (scrambled, Sigma) by using Lipofectamine 2000 (Invitrogen, USA), according to manufacturer instructions. siRNA1: sense: 5'-CGACACUGUCAUGAAUGAGUCUGAA-3'; antisense: 5'-UUCAGACUCAUUCAUGACAGUGUCG -3'. siRNA2: sense: 5'-ACACUGACAACUGUCGAGAAGUGAU -3'; antisense: 5'-AUCACUUCUCGACAGUUGUCAGUGU -3'. Silencing was confirmed by Western Blotting by using a mouse anti-GRASP55 polyclonal antibody (ab68713, Abcam) at a 1/200 dilution (Supplemental Figure 8). Electrophysiological and Western Blot analyses were performed 24 h after transfection. In another group of experiments, rat ventricular

or iCell²® hiPSC-derived cardiomyocytes were infected with lentiviral constructs encoding for GRASP55 (NM_001007720) (A: 5'-AGTCTGAAGACCTGTTTCAGCCTTATTGAG-3' and B: 5'-AGACCTCACAGCGATTACATCATTGGAGC-3') and GRASP65 (NM_019385) (A: 5'-AGTCGGAAGACTTCTTCACTCTCATTGAG-3' and B: 5'-GCACTGCTGAAGGCTAATGTGGAGAAGCC-3') silencing shRNA together with GFP or with a scrambled shRNA (Origene Technologies, Inc. USA). Lentivirus encoding shRNA constructs were amplified, purified, and titered using previously described protocols (1). For GRASP silencing, MOI= 30 and 80 were used for shRNA GRASP and scrambled lentiviral constructs, respectively. The same stock of shRNA GRASP constructs and scrambled shRNA was used for all of the experiments. A group of cultured rat ventricular or iCell²® hiPSC-derived cardiomyocytes were co-infected with lentivirus encoding shRNA GRASP and with adenovirus encoding Nav1.5WT. To ensure the efficiency of the infection of both viral vectors, they were incubated two hours apart. In all cases, I_{Na} and I_{K1} were also recorded 48 h after the infection; infected cells were identified by GFP fluorescence under fluorescent microscopy (Nikon Eclipse TE2000S, Nikon). Silencing of GRASP expression was confirmed in cultured rat ventricular myocytes by Western blot 48 h after the infection by using a rabbit anti-GRASP55 polyclonal antibody (ab74579, Abcam) at a 1/500 dilution (Supplemental Figure 8).

Immunofluorescence and imaging (14).

COS7 cells were grown in Dulbecco's modified Eagle's medium (DMEM) supplemented with 10% fetal bovine serum at 37 °C in an atmosphere of 5% CO₂. Cells were transiently transfected with pD1690N-GFP or pG1748D-GFP Nav1.5 mutants

(0.5 µg) alone or with the Golgi marker mCherry-Golgi-7 (Addgene) (0.5 µg) by using Eugene XtremeGENE and then incubated for 24 h at 37 °C, trypsinized, and seeded on coverslips at low density (100,000 cells/P35 dish). Twenty four hours later, coverslips were transferred to multiwell dishes, rinsed twice with phosphate buffered saline solution (PBS) and fixed (2 min) in 2% paraformaldehyde/PBS followed by cold methanol (-20 °C, 10 min). To detect calnexin cells were blocked with 0.2 M glycine (pH=8.0) for 5 min and 0.5% Bovine serum albumin in PBS for 30 min. Overnight incubation at 4 °C or for 2 h at 37 °C with anti-Calnexin-CT antibody 1:200 (StressMarq, SPC-108) was done in PBS. After three washes cells were incubated for 1 h with anti-rabbit Alexa-647 1:500 (ThermoFischer) diluted in PBS, and 5 min with 4',6-Diamidino-2-phenylindole dihydrochloride (DAPI) 1:5.000 (Merck). Coverslips were mounted in mowiol and imaged using a Zeiss AxioVert 200M fluorescence microscope equipped with 40X Plan Neofluar NA 1.3 or 63X PlanApo NA 1.4 objectives, a CoolLED pE-4000 light source, Coolsnap FX mono camera and MetaMorph software. Digital image processing (background subtraction, shading correction) and montage were performed using ImageJ (<http://rsb.info.nih.gov/ij/>) (15). Colocalization between the mutant Na channels and ER (Calnexin) or Golgi (mCherry-Golgi) markers was measured in each experimental group by using BioimageXD (<http://www.bioimagexd.net/>) (3).

Statistics.

Results are expressed as mean±SEM. Unpaired t-test or one-way ANOVA followed by Newman-Keuls test were used where appropriate. In small-size samples (n<15), statistical significance was confirmed by using nonparametric tests. To take into

account repeated sample assessments, data were analyzed with multilevel mixed-effects models. A value of $P < 0.05$ was considered significant.

Study approval.

Animal studies were approved by the University Committees on the Use and Care of animals at the Complutense University and the University of Michigan and conformed to the Guidelines from Directive 2010/63/EU of the European Parliament on the protection of animals used for scientific purposes.

Supplemental References

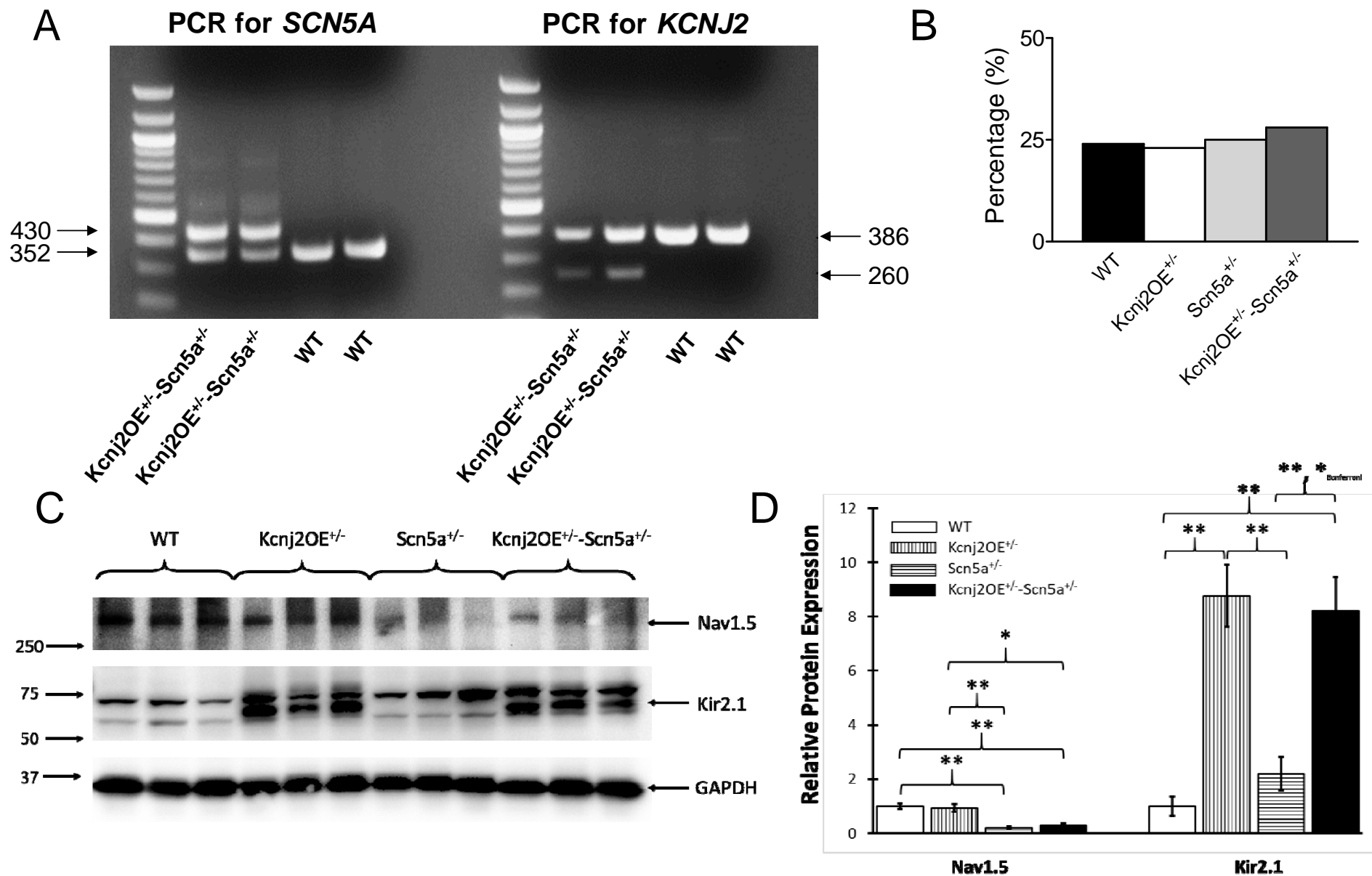
1. Matamoros M, et al. Nav1.5 N-terminal domain binding to α 1-syntrophin increases membrane density of human Kir2.1, Kir2.2 and Nav1.5 channels. *Cardiovasc Res.* 2016;110(2):279-290.
2. Núñez L, et al. p.D1690N Nav1.5 rescues p.G1748D mutation gating defects in a compound heterozygous Brugada syndrome patient. *Heart Rhythm.* 2013;10(2):264-272.
3. Dolz-Gaitón P, et al. Functional characterization of a novel frameshift mutation in the C-terminus of the Nav1.5 channel underlying a Brugada syndrome with variable expression in a Spanish family. *PLoS One.* 2013;8(11):e81493.
4. Caballero R, et al. Tbx20 controls the expression of KCNH2 gene and of hERG channels. *Proc Natl Acad Sci USA.* 2017;114(3):E416-E425.
5. Gómez R, et al. Structural basis of drugs that increase cardiac inward rectifier Kir2.1 currents. *Cardiovasc Res.* 2014;104(2):337-346.
6. Amorós I, et al. Propafenone blocks human cardiac Kir2.x channels by decreasing the negative electrostatic charge in the cytoplasmic pore. *Biochem Pharmacol.* 2013;86(2):267-278.
7. Gómez R, et al. Nitric oxide increases cardiac I_{K1} by nitrosylation of cysteine 76 of Kir2.1 channels. *Circ Res.* 2009;105(4):383-392.
8. Caballero R, et al. Flecainide increases Kir2.1 currents by interacting with cysteine 311, decreasing the polyamine-induced rectification. *Proc Natl Acad Sci USA.* 2010;107(35):15631-15636.
9. Piao L, Li J, McLerie M, Lopatin AN. Transgenic upregulation of I_{K1} in the mouse heart is proarrhythmic. *Basic Res Cardiol.* 2007;102(5):416–428.

10. Liu K, et al. Recombinase-mediated cassette exchange to rapidly and efficiently generate mice with human cardiac sodium channels. *Genesis*. 2006;44(11):556-564.
11. Papadatos GA, et al. Slowed conduction and ventricular tachycardia after targeted disruption of the cardiac sodium channel gene *Scn5a*. *Proc Natl Acad Sci USA*. 2002;99(9):6210-6215.
12. Milstein ML, et al. Dynamic reciprocity of sodium and potassium channel expression in a macromolecular complex controls cardiac excitability and arrhythmia. *Proc Natl Acad Sci USA*. 2012;109(31):E2134-E2143.
13. Herron TJ, et al. Extracellular Matrix-Mediated Maturation of Human Pluripotent Stem Cell-Derived Cardiac Monolayer Structure and Electrophysiological Function. *Circ Arrhythm Electrophysiol*. 2016;9(4):e003638.
14. Garrido-García A, Andrés-Pans B, Durán-Trío L, Díez-Guerra FJ. Activity-dependent translocation of neurogranin to neuronal nuclei. *Biochem J*. 2009;424(3):419-429.
15. Schneider CA, Rasband WS, Eliceiri KW. NIH Image to ImageJ: 25 years of image analysis. *Nat Methods*. 2012;9(7):671-675.

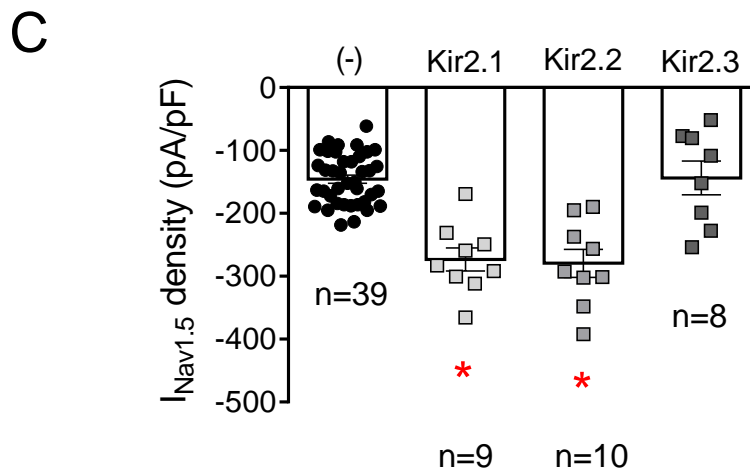
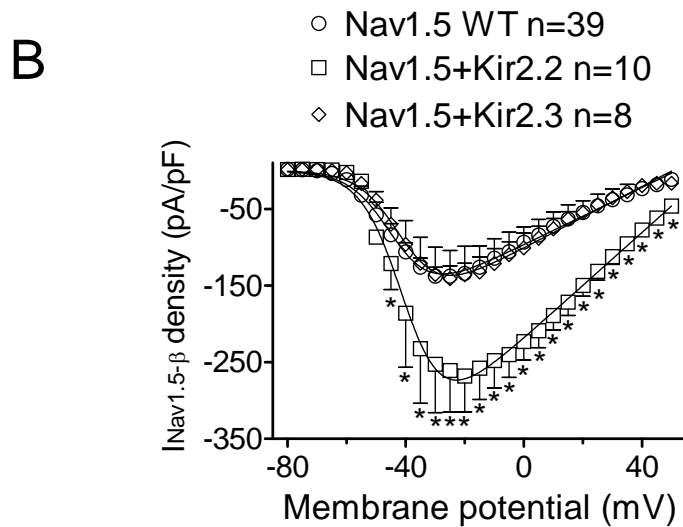
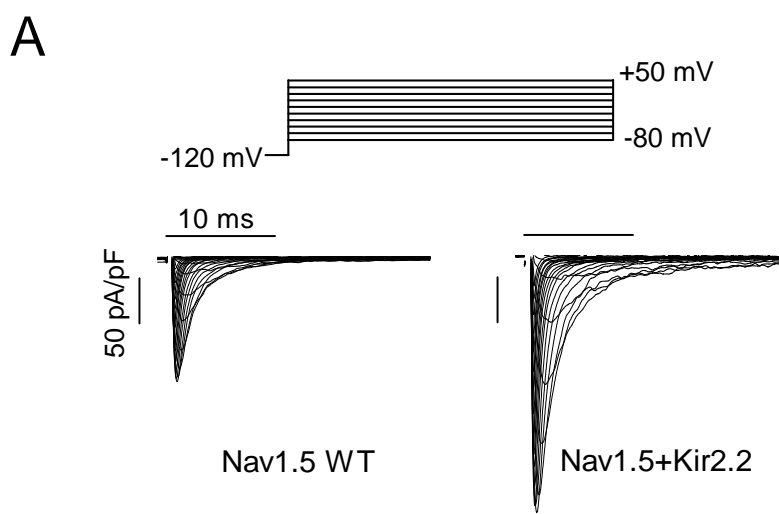
Supplemental Table 1. Effects of the trafficking-deficient Nav1.5 mutants on the voltage dependence of activation (conductance-voltage curves) and inactivation of the I_{Na} recorded in rat ventricular myocytes.

	Conductance-voltage		Inactivation	
	V _h (mV)	<i>k</i>	V _h (mV)	<i>k</i>
Ad-GFP	-57.9±1.1	4.3±0.1	-91.7±1.5	5.7±0.3
Ad-Nav1.5	-56.8±0.6	4.2±0.1	-90.0±0.9	5.7±0.5
Ad-p.G1748D	-54.2±1.1*	4.5±0.2	-85.7±2.1*	5.4±0.3
Ad-p.D1690N	-56.1±1.3	4.7±0.2	-91.1±1.4	5.7±0.2
Ad-p.D1816fs	-54.6±1.0*	4.6±0.2	-84.2±2.3*	5.4±0.2

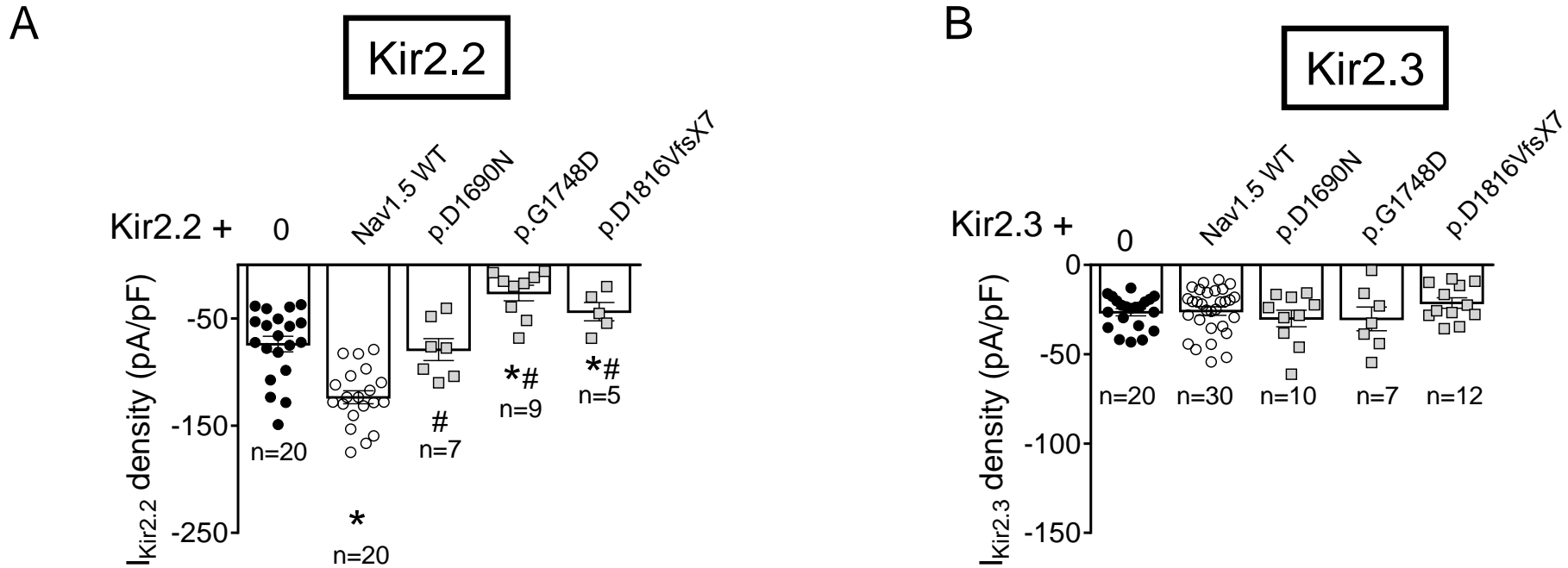
V_h and *k*= midpoint and slope values of the curves. * P<0.05 vs Ad-GFP infected myocytes



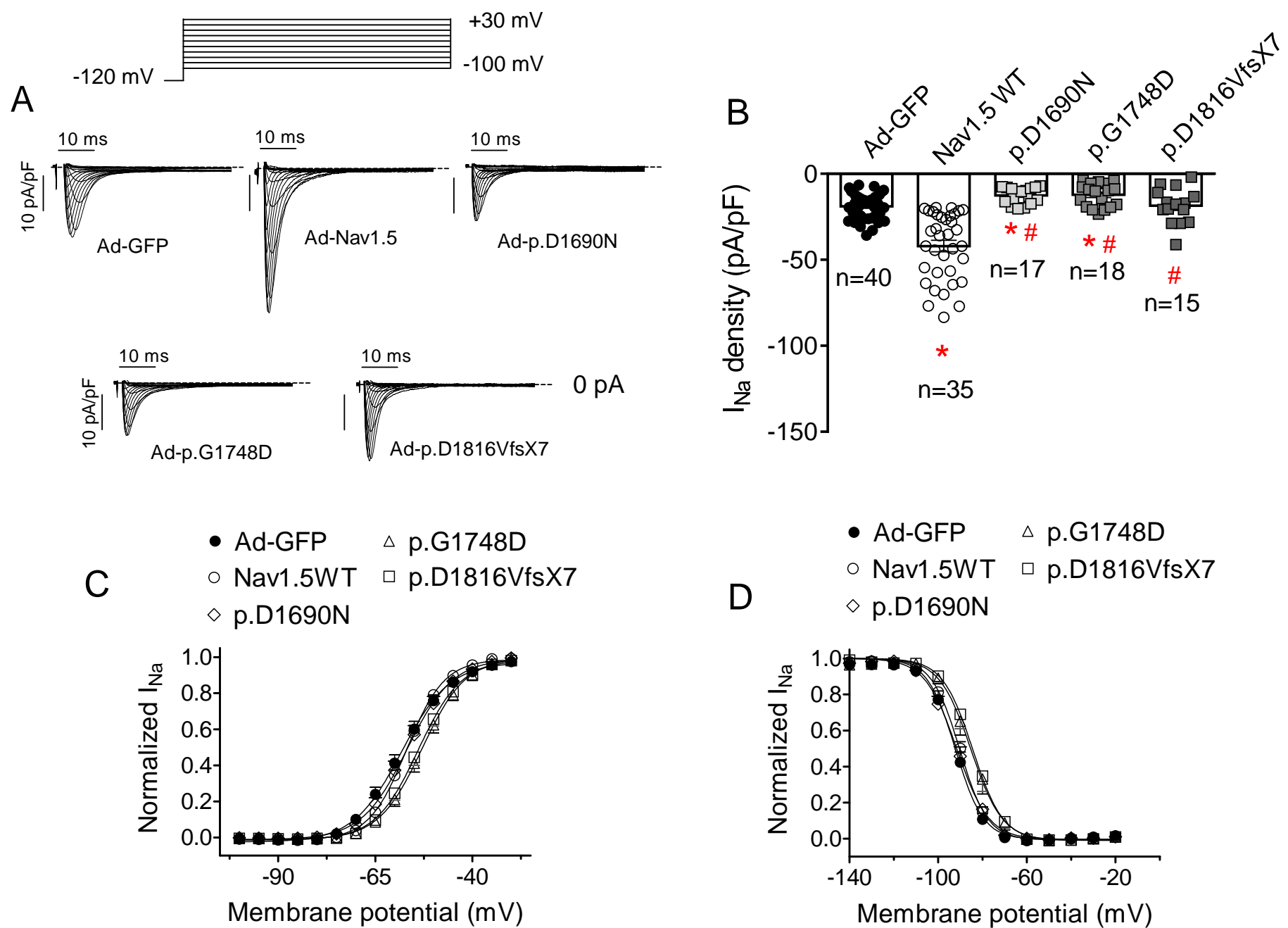
Supplemental Figure 1. Successful crossbreeding of *Scn5a*^{+/-} mice with *Kcnj2OE*^{+/-} mice. (A) End point PCR profile in WT and *Kcnj2OE*^{+/-} - *Scn5a*^{+/-} mice obtained when crossing *Scn5a*^{+/-} with *Kcnj2OE*^{+/-} mice by using specific primers for detecting *KCNJ2* (right) and *SCN5A* (left). Overexpression of *KCNJ2* fused to GFP was only observed in *Kcnj2OE*^{+/-} - *Scn5a*^{+/-} mice (lower band corresponding to 260 bp fragment), whereas a 386 bp fragment corresponding to native *KCNJ2* was amplified in both groups. *SCN5A* was knocked by using Cre-recombinase mediated cassette exchange with GFP in the targeted locus. This resulted in the appearance of a 430 bp fragment only in *Kcnj2OE*^{+/-} - *Scn5a*^{+/-} mice that indicates the *SCN5A* knockout allele. The 352 bp fragment corresponds to genomic mouse *SCN5A*, amplified in WT and *Kcnj2OE*^{+/-} - *Scn5a*^{+/-} mice. (B) Mendelian inheritance observed among WT, *Kcnj2OE*^{+/-}, *Scn5a*^{+/-} and *Kcnj2OE*^{+/-} - *Scn5a*^{+/-} mice (N=88 newborn mice). As can be observed, cross-breeding of *Scn5a*^{+/-} and *Kcnj2OE*^{+/-} mice was successful as demonstrated by PCR (Panel A). On the other hand, the genetic distribution of these mice was that of Mendelian inheritance with a 25% probability of obtaining each of the four groups with no evidence of embryonic death (Panel B). (C) Representative Western blot images showing the expression of Nav1.5 and Kir2.1 in ventricle lysates from WT, *Kcnj2OE*^{+/-}, *Scn5a*^{+/-} and *Kcnj2OE*^{+/-} - *Scn5a*^{+/-} mice hearts. (D) Densitometric analysis of the Nav1.5 (left) and Kir2.1 (right) expression normalized to GAPDH expression. Results are expressed as mean signal intensity (N = 3 per genotype, *P < 0.05, mean±SEM). As can be observed in panels C and D, the expression of Nav1.5 was significantly reduced in *Scn5a*^{+/-} and *Kcnj2OE*^{+/-} - *Scn5a*^{+/-} mice. On the other hand, Kir2.1 expression was markedly increased in *Kcnj2OE*^{+/-} and *Kcnj2OE*^{+/-} - *Scn5a*^{+/-} mice compared to both WT and *Scn5a*^{+/-} mice. One way ANOVA followed by Newman-Keuls and multilevel mixed-effects model were used for comparisons.



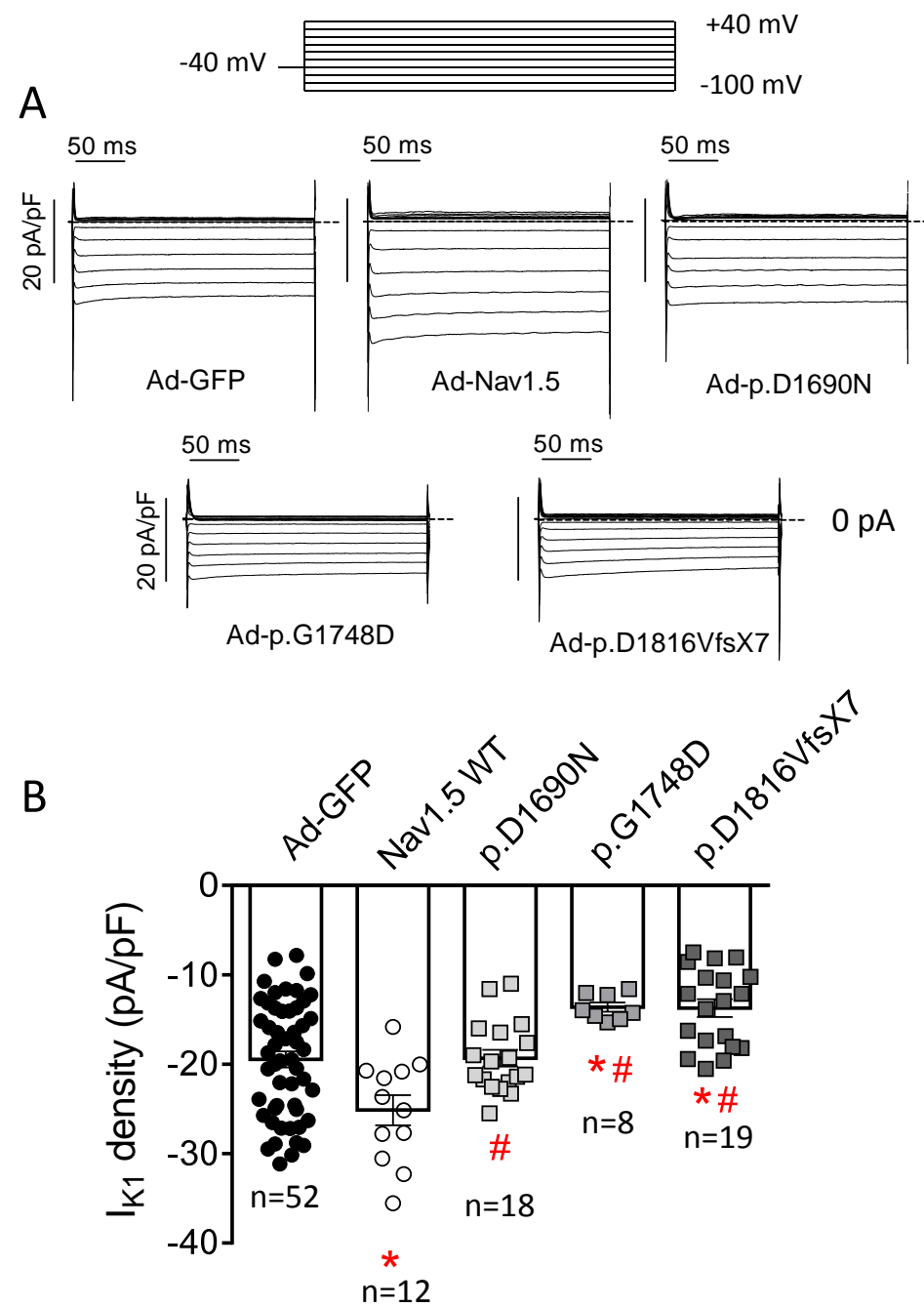
Supplemental Figure 2. Positive reciprocal modulation between Nav1.5 and Kir2.1/2.2 channels. (A) $I_{Nav1.5}$ traces obtained by applying the protocol shown at the top in CHO cells transfected with Nav1.5 channels alone (1.6 μ g) or together with Kir2.2 channels (1.6+1.6 μ g). (B) Mean current density-voltage curves for $I_{Nav1.5}$ recorded in cells expressing Nav1.5 alone or together with Kir2.2 or Kir2.3 channels. Each data point represents the mean \pm SEM of "n" cells from at least three different batches. (C) Peak $I_{Nav1.5}$ density recorded in cells expressing Nav1.5 alone or together with Kir2.1, Kir2.2, or Kir2.3 channels. Each bar represents the mean \pm SEM of "n" cells from at least three different batches and each dot represents one cell. * P <0.05 vs Nav1.5 WT alone. One way ANOVA followed by Newman-Keuls and multilevel mixed-effects model were used for comparisons. In panels A and B, it can be observed that cotransfection with Kir2.2 channels significantly increased the $I_{Nav1.5}$ density at all the voltages tested ($n \geq 10$, $P < 0.05$). Moreover, positive $I_{Nav1.5}$ modulation produced by Kir2.2 channels was indistinguishable from that produced by Kir2.1 channels (Panel C). On the other hand, Kir2.3 channels did not positively modulate $I_{Nav1.5}$ at any of the voltages tested (Panel B) and, thus, the $I_{Nav1.5}$ generated when Kir2.3 and Nav1.5 channels were coexpressed was similar to that generated by Nav1.5 channels alone (Panels B and C).



Supplemental Figure 3. Effects of trafficking-defective Nav1.5 mutants on $I_{Kir2.2}$ and $I_{Kir2.3}$. (A and B) $I_{Kir2.2}$ (A) and $I_{Kir2.3}$ (B) density at -120 mV generated in CHO cells transfected with Kir2.2 (A), and Kir2.3 (B) channels alone or together with WT or p.D1690N, p.G1748D, and p.D1816VfsX7 Nav1.5 channels. Each bar represents the mean \pm SEM of "n" cells from at least three different batches and each dot represents one cell. * $P < 0.05$ vs Kir2.2 alone; # $P < 0.05$ vs Kir2.2+Nav1.5WT. One way ANOVA followed by Newman-Keuls and multilevel mixed-effects model were used for comparisons. Cotransfection with Nav1.5 channels significantly increased the current generated by Kir2.2 ($I_{Kir2.2}$) but not that generated by Kir2.3 ($I_{Kir2.3}$) channels (Panels A and B). Interestingly, $I_{Kir2.2}$ density was not modified when Kir2.2 channels were cotransfected with p.D1690N but was significantly reduced when they were cotransfected with p.G1748D and p.D1816VfsX7 Nav1.5 mutant channels compared to that generated by Kir2.2 channels alone ($n \geq 5$, $P < 0.05$) (Panel A). On the other hand, $I_{Kir2.3}$ density was not modified when Kir2.3 channels were cotransfected with any of the three trafficking-defective Nav1.5 mutants tested (Panel B).

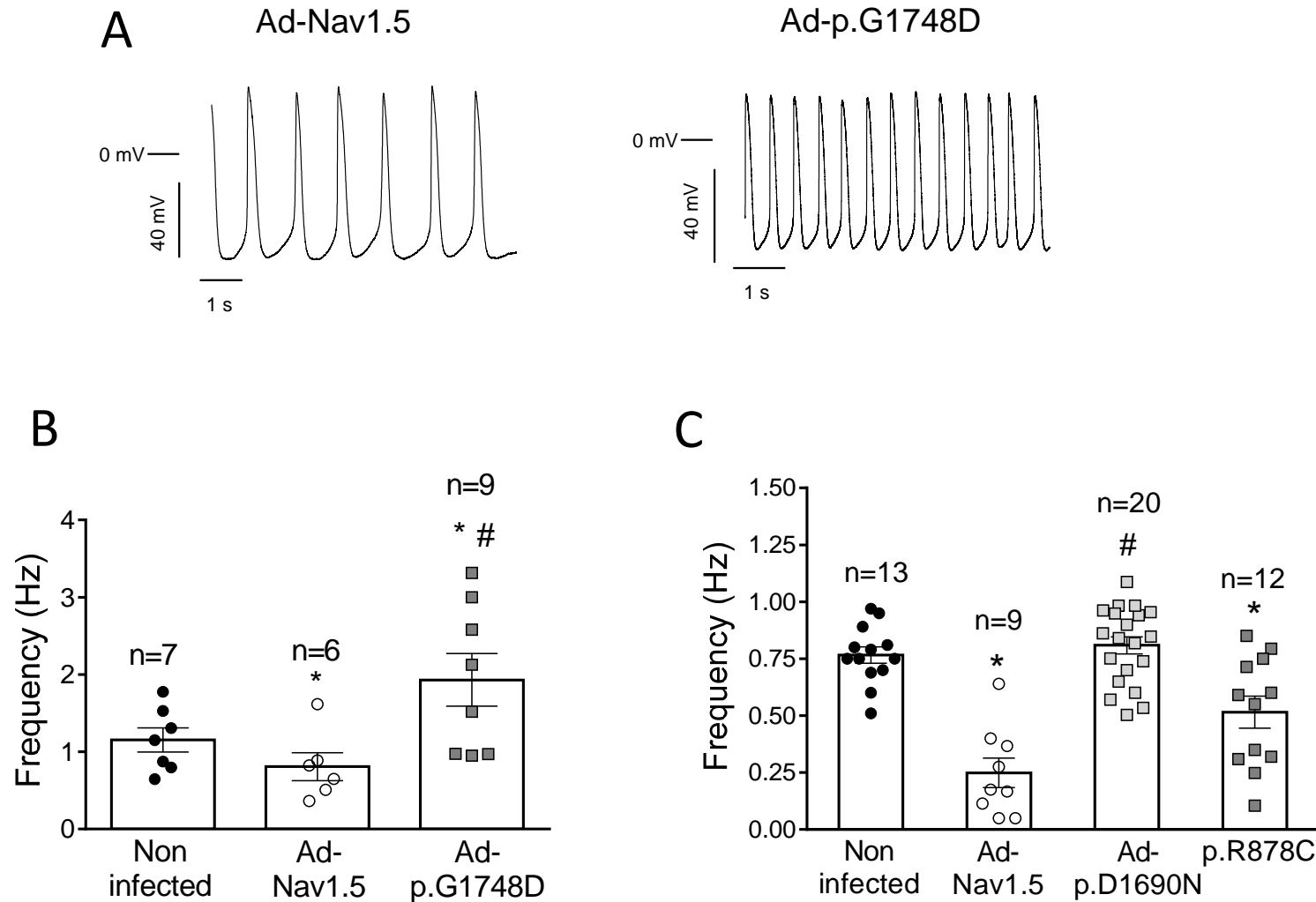


Supplemental Figure 4. Effects of trafficking-defective Nav1.5 mutants on the I_{Na} recorded in rat ventricular CMs. (A) I_{Na} traces recorded by applying the protocol shown at the top in ventricular CMs infected with the adenoviral (Ad) constructions encoding for GFP only (Ad-GFP), or for WT and mutated Nav1.5 channels. (B) Peak I_{Na} density recorded in CMs obtained from 8 rats infected with the adenoviral constructions. (C and D) Conductance-voltage (C) and inactivation (D) curves constructed for CMs infected with the adenoviral constructions. In A, dashed lines represent the zero current level. In C and D, continuous lines represent the fit of a Boltzmann equation to the data. Results are expressed as mean \pm SEM of "n" myocytes and each dot (Panel B) represents one myocyte. * $P < 0.05$ vs Ad-GFP, # $P < 0.05$ vs Ad-Nav1.5 WT. One way ANOVA followed by Newman-Keuls and multilevel mixed-effects model were used for comparisons.



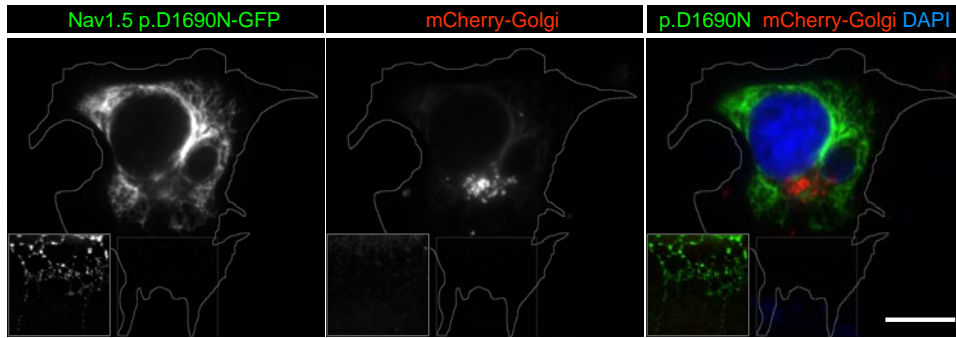
Supplemental Figure 5. Effects of trafficking-defective Nav1.5 mutants on the I_{K1} recorded in rat ventricular CMs. (A) I_{K1} traces recorded by applying the protocol shown at the top in ventricular CMs infected with Ad-GFP or for WT and mutated Nav1.5 channels. Dashed lines represent the zero current level. (B) I_{K1} density at -120 mV recorded in CMs obtained from 8 rats infected with the adenoviral constructs. In B, results are expressed as mean \pm SEM of "n" myocytes and each dot represents one myocyte. * $P < 0.05$ vs Ad-GFP, # $P < 0.05$ vs Ad-Nav1.5 WT. One way ANOVA followed by Newman-Keuls and multilevel mixed-effects model were used for comparisons.

Spontaneous action potentials in hiPSC-CM

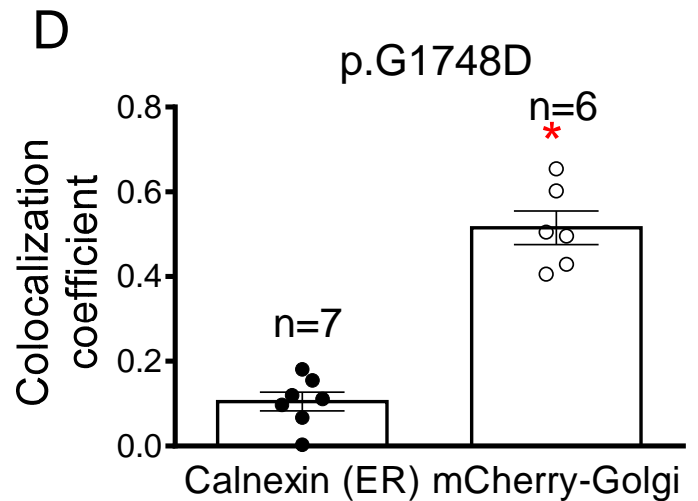
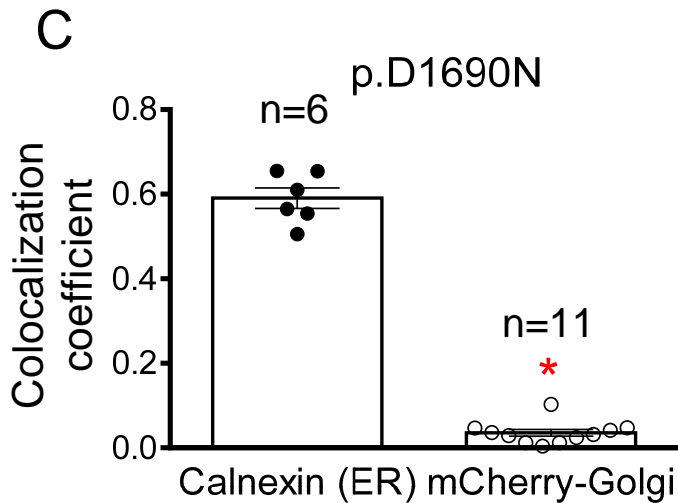
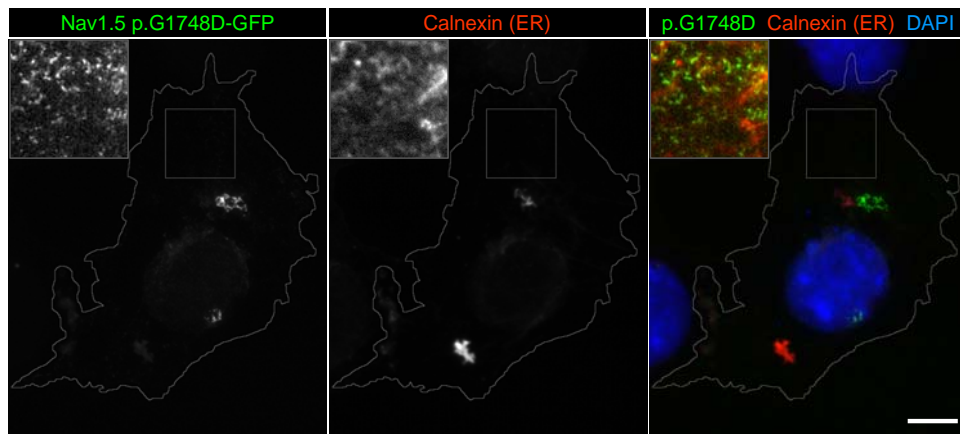


Supplemental Figure 6. Effects of trafficking defective mutants on automatic firing frequency for APs recorded in hiPSC-CMs. (A) Series of spontaneous APs recorded in hiPSC-CM infected with Ad-Nav1.5 (left) or Ad-p.G1748D (right). (B) Firing frequency for APs recorded in DF19-9-11T hiPSC-CMs infected or not with Ad-Nav1.5 or Ad-p.G1748D. (C) Firing frequency for APs recorded in iCell² hiPSC-CMs infected or not with Ad-Nav1.5 or Ad-p.D1690N or transfected with p.R878C Nav1.5. In B and C results are expressed as mean \pm SEM of "n" experiments from at least 5 different dishes and each dot represents one cell. *P<0.05 vs non-infected; #P<0.05 vs Ad-Nav1.5. One way ANOVA followed by Newman-Keuls and multilevel mixed-effects model were used for comparisons. As shown in the Figure, in both types of hiPSC-CMs infection with Ad-Nav1.5 significantly reduced the automatic firing frequency. Conversely, infection with Ad-p.G1748D and Ad-p.D1690N significantly increased the firing frequency (Panels B and C). Interestingly, transfection of the cDNA encoding p.R878C Nav1.5 channels, which increase the $I_{Kir2.1}$ density, also significantly decreased firing frequency (Panel C).

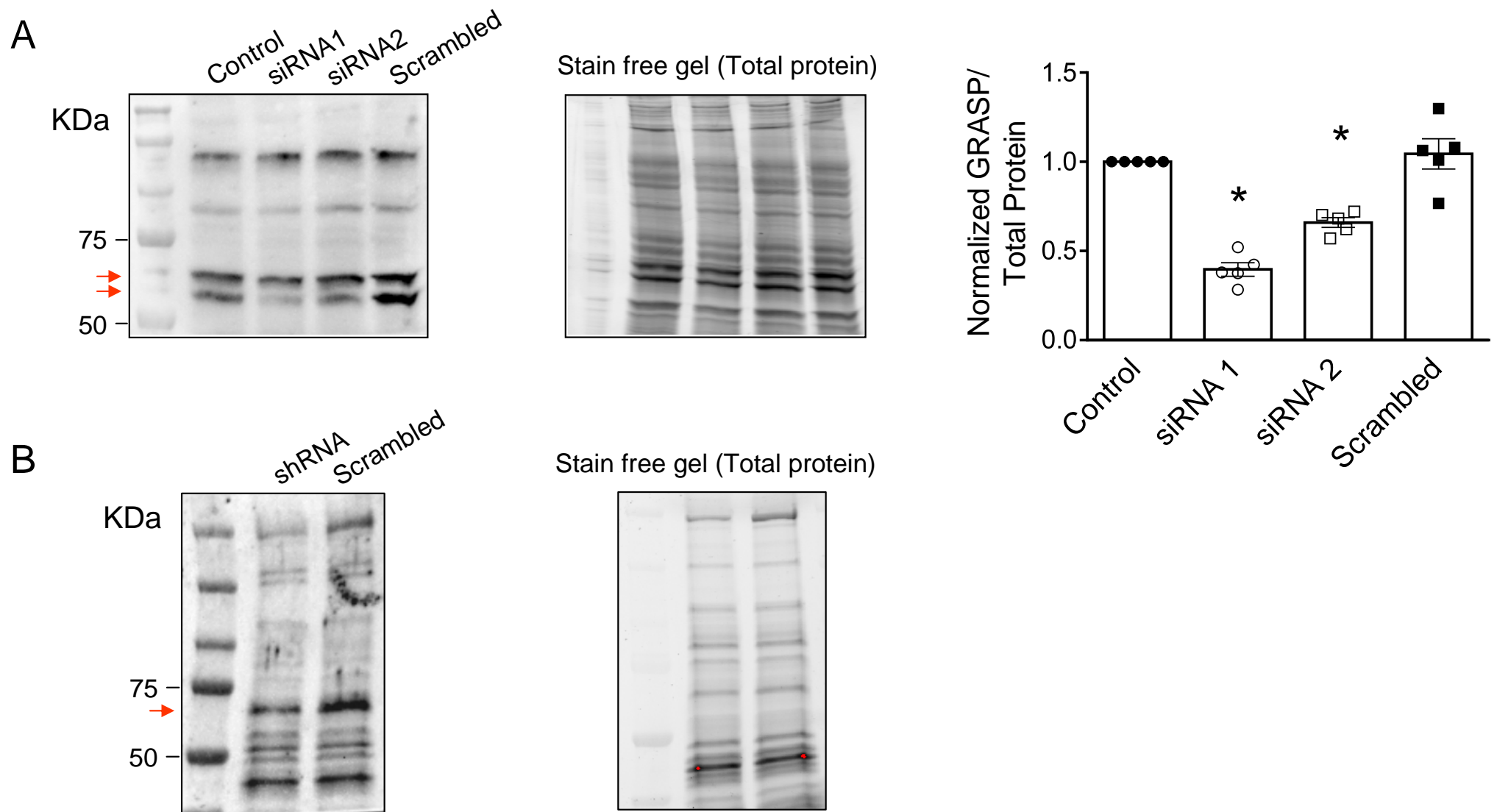
A p.D1690N Nav1.5



B p.G1748D Nav1.5



Supplemental Figure 7. p.D1690N and p.G1748D do not co-localize with Golgi and ER markers, respectively. (A) Representative cell expressing p.D1690N-GFP Nav1.5 channels and mCherry-Golgi. (B) Intracellular localization analysis of p.G1748D-GFP Nav1.5 channels and the ER marker Calnexin. Cell contours are outlined in grey for enhanced visualization. Insert images are included to make highlighted low contrast regions visible. Scale bars = 25 μ m. (C and D) Colocalization coefficients for p.D1690N (C) and p.G1748D (D) with the ER marker Calnexin and mCherry-Golgi. In C and D, bars represent mean \pm SEM of "n" cells from at least 3 different batches and each dot represents one cell. * $P < 0.05$ vs colocalization with Calnexin. Unpaired t -test and multilevel mixed-effects model were used. As can be observed in Panels A and C, p.D1690N-GFP and mCherry-Golgi displayed a markedly different intracellular distribution pattern and no co-localization was observed between them. This result can be explained considering that p.D1690N resided and in most cells accumulated in the ER. Interestingly, expression of p.G1748D led to a noticeable stress at the ER. Indeed, cells expressing p.G1748D-GFP often displayed an altered Calnexin distribution pattern, featuring strongly immunoreactive accumulations (local clumps) and decreased levels in the ER network. Importantly, there is no overlap between p.G1748D Nav1.5 channels and Calnexin in either location (Panels B and D).

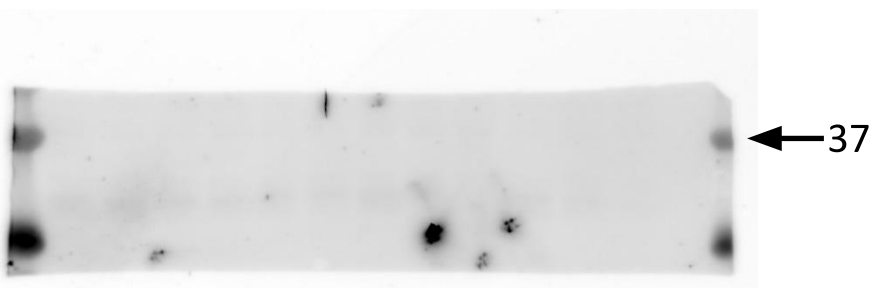
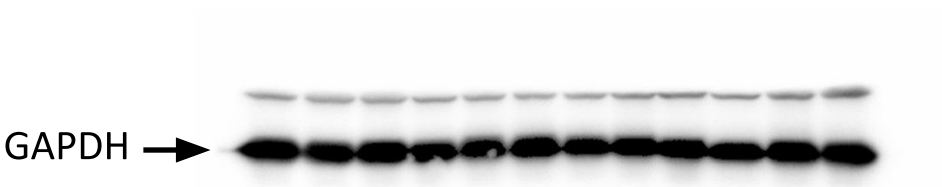
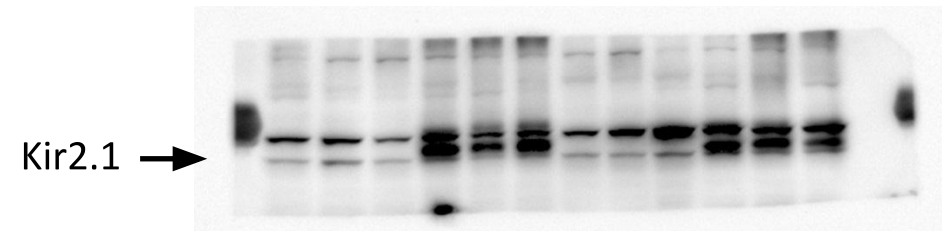
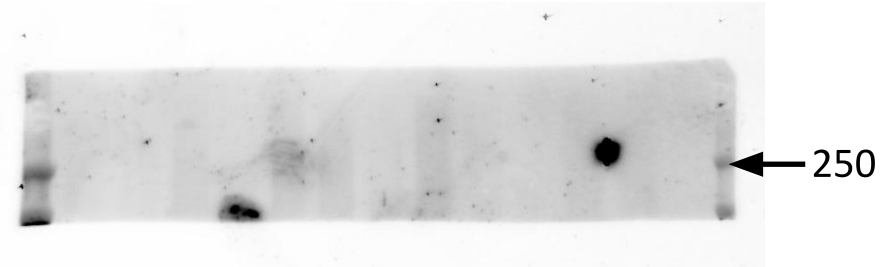
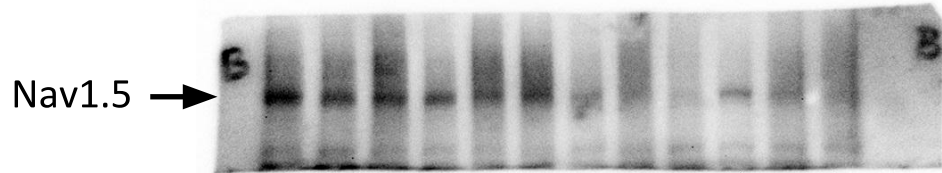


Supplemental Figure 8. GRASP silencing in CHO cells and rat ventricular myocytes. (A) GRASP55 immunoblot (arrows) of CHO cells transfected or not with two different GRASP55-specific siRNAs or with a negative control (Scrambled) (left). The corresponding Stain-free gel is depicted to show the total protein. Each lane corresponds to a dish of cells transfected or not with scrambled or siRNA GRASP55. Expression of GRASP55 normalized to the total protein measured by Western blot in CHO cells transfected or not with GRASP55 specific siRNAs or a scrambled siRNA is shown in the right panel. Results are expressed as mean \pm SEM signal intensity, and they represent data from five dishes in each condition. * $P < 0.05$ vs cells transfected with scrambled siRNA. One-way ANOVA followed by Newman-Keuls and multilevel mixed-effects model were used for comparisons. Transfection of both siRNA1 and siRNA2 for 24 h led to significant reduction of GRASP55 in CHO cells, which reached a $\approx 65\%$ with siRNA1. For this reason, this was the siRNA construct selected for GRASP55 silencing in the electrophysiological experiments. (B) GRASP55 immunoblot (arrow) of rat ventricular CMs infected with GRASP55/65-specific shRNA or with a negative control (Scrambled) (left). The corresponding Stain-free gel is depicted to show the total protein (right). Each lane corresponds to a dish of cells infected with scrambled or shRNA GRASP55/65.

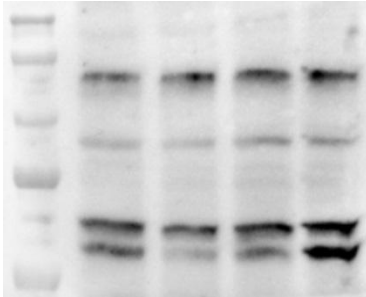
Membranes uncropped/unedited Supp. Figure 1 C

Chemi Hi Resolution channel

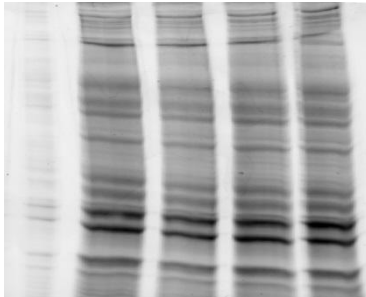
IRDye 680 channel (markers)



Supp. Figure 8A



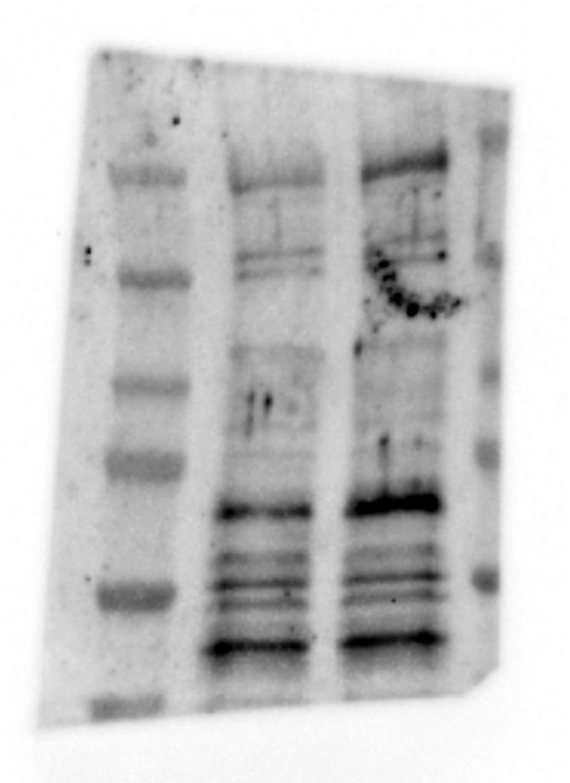
Uncropped membrane



Total protein Gel

Supp. Figure 8B

Uncropped membrane



Total protein Gel

